SURFACE AND INTERFACE ANALYSIS
Surf. Interface Anal. 2004; **36**: 977–980
Published online in Wiley InterScience (www.interscience.wiley.com). DOI: 10.1002/sia.1816

SIA

Surface characterization of the oxide layer grown on Ti–Nb–Zr and Ti–Nb–Al alloys

A. Gutiérrez,[1]* M. F. López,[2] J. A. Jiménez,[3] C. Morant,[1] F. Paszti[4,†] and A. Climent[1,4]

[1] Departamento de Física Aplicada, Universidad Autónoma de Madrid, Cantoblanco, E-28049 Madrid, Spain
[2] Instituto de Ciencia de Materiales de Madrid, CSIC, Cantoblanco, E-28049 Madrid, Spain
[3] Centro Nacional de Investigaciones Metalúrgicas, CSIC, Av. Gregorio del Amo 8, E-28040 Madrid, Spain
[4] Centro de Microanálisis de Materiales, Cantoblanco, E-28049 Madrid, Spain

Received 28 July 2003; Revised 27 November 2003; Accepted 27 November 2003

The surface of the oxide layers formed after oxidation in air at 750 °C of three titanium alloys has been characterized by several techniques. The investigated alloys were Ti–7Nb–6Al, Ti–13Nb–13Zr and Ti–15Zr–4Nb, with potential applications as biomaterials. XPS experiments showed that, after 24 h exposure, the surface of the Ti–7Nb–6Al alloy is mainly formed of Al_2O_3, with a minor presence of TiO_2, and absence of Nb oxide. On the other hand, the surface of both Ti–Nb–Zr alloys is mainly composed of TiO_2, with some amount of ZrO_2 and Nb_2O_5. An enrichment of the Nb signal is observed in both samples with respect to the bulk composition. The topography and surface morphology of the oxidized alloys were investigated by atomic force microscopy. A more regular surface topography was observed for the Ti–7Nb–6Al alloy than for the Ti–Nb–Zr alloys and, consequently, a higher potentiality in biomedical applications. Finally, in order to get in-depth information of the oxide scale, Rutherford backscattering spectroscopy experiments were also performed. The results obtained with this technique confirm those obtained by XPS, and can help to understand the mechanism and kinetics of the oxide film formation.

KEYWORDS: titanium alloys; oxidation; XPS; RBS; atomic force microscopy; biomaterials

INTRODUCTION

Commercially pure titanium as well as the Ti–6Al–4V alloy are conventional biomaterials widely used because of their biocompatibility and corrosion resistance.[1,2] However, there exists a scientific controversy on the cytotoxicity of elemental vanadium.[3,4] For this reason, new vanadium-free Ti alloys are currently being evaluated for biomedical applications.[5–8]

The biocompatibility of metallic biomaterials strongly depends on the ion release caused by the corrosion process in the presence of the physiological human fluid. Implant alloys are materials that typically feature the formation of a native surface oxide film, the passive layer, which protects them from corrosion. The protective character of this passive layer depends on several properties, such as compactness, film continuity, ionic conductivity, etc. Pure titanium, as well as titanium alloys, exhibits excellent biocompatibility as a consequence of the highly protective character of the passive layer.

The native oxide formed on Ti alloys consists of a mixture of different titanium sub-oxides as well as other oxides that depend on the Ti alloy composition.[8] A possibility to improve the corrosion resistance of these alloys and, therefore, their biocompatibility, is to increase the thickness of the surface oxide layer. This can be made by high-temperature oxidation, which, in general, promotes Ti diffusion to the surface, reducing thus the presence of non-protective oxides. This procedure usually leads to an increase in the corrosion resistance with respect to the native oxide layer.

The objective of this work is to perform a surface characterization of three different vanadium-free titanium alloys, Ti–6Al–7Nb, Ti–13Nb–13Zr and Ti–15Zr–4Nb, after an oxidation treatment at 750 °C for 24 h. The composition of the outer layers of the oxide films formed on the alloys during the thermal process was determined by XPS. Additionally, the topography and surface morphology of the oxide layer, also important for using these materials in biomedical applications, were studied by atomic force microscopy (AFM). Finally, in order to get more insight into the mechanisms and kinetics of the oxide film formation, Rutherford backscattering spectroscopy (RBS) and elastic recoil detection (ERD) experiments were also performed, giving in-depth information of the oxide scale.

*Correspondence to: A. Gutiérrez, Departamento de Física Aplicada, Universidad Autónoma de Madrid, Cantoblanco, E-28049 Madrid, Spain. E-mail: a.gutierrez@uam.es
†On leave from the KFKI Research Institute for Particle and Nuclear Physics, Budapest, Hungary
Contract/grant sponsor: Programa de Tecnología de los Materiales de la Comunidad Autónoma de Madrid, Spain; Contract/grant number: 07N-0050-1999.
Contract/grant sponsor: Ministerio de Ciencia y Tecnología, Spain.
Contract/grant sponsor: Ministerio de Educacion, Cultura y Deporte; Contract/grant number: SAB2000-0243.

EXPERIMENTAL

The chemical compositions, in wt%, of the three titanium alloys were: Ti–7Nb–6Al, Ti–13Nb–13Zr and Ti–15Zr–4Nb, which in at.% correspond to $Ti_{85.9}Al_{10.5}Nb_{3.6}$, $Ti_{84.5}Nb_{7.7}Zr_{7.8}$ and $Ti_{89.1}Zr_{8.7}Nb_{2.3}$, respectively. These alloys were prepared by arc melting and then casting in a copper coquille under high vacuum. The specimens were cut from as-cast ingots by electrospark-erosion. With the aim of obtaining a two-phase ($\alpha + \beta$) microstructure, which ensures satisfactory mechanical properties, the alloys were annealed above the β-transition temperature at 1100 °C for 1 h and aged at 700 °C for 1 h. The samples were abraded and polished using diamond pastes of successively finer particle size. In the final stage of this process, colloidal silica was used to ensure a surface free of mechanical deformation. Then, the samples were ultrasonically cleaned in acetone. Finally, the samples were isothermally oxidized at 750 °C in air for 24 h.

The chemical composition of the oxide layers formed on the titanium alloys was studied by XPS, RBS and ERD. The XPS spectra were recorded under ultra-high vacuum (UHV) conditions with a VG-CLAM hemispherical electron energy analyser using Mg K_α x-rays as the excitation source. Previously to the measurements, sample surfaces were cleaned by ion sputtering using 5 keV Ar ions for 1 min. For such short sputtering time, possible side-effects, such as changes in the surface composition and roughness, are not relevant for the conclusions of this work. XPS spectra were then analysed by a least-squares-fit procedure using standard Gaussian–Lorentzian lines and the corresponding integral background.

RBS and ERD measurements were carried out using the new 5 MeV tandem accelerator of the Centro de Microanálisis de Materiales (CMAM), at the Parque Científico de Madrid. For RBS, the energy of the analysing He^+ ions was 2 MeV, and 5.61 MeV, respectively. At the latter energy the analysed depth reached 4×10^{19} atoms/cm^2 and the sensitivity for oxygen and carbon increased by two orders of magnitude. The samples were also characterized by ERD using 28 MeV Si^{5+} ions. The measurements were evaluated by the RBX code.[9]

AFM measurements were performed under ambient conditions and in contact mode with a commercial microscope[10] using rectangular Si_3N_4 cantilevers (NT-MTD, 0.6 N/m nominal spring constant).

RESULTS AND DISCUSSION

Figure 1 shows Ti 2p core-level emission of the three oxidized alloys. The dashed sub-spectra represent the signal corresponding to the Ti $2p_{3/2}$ emission and the dotted curves represent the Ti $2p_{1/2}$ emission, with a spin-orbit splitting of 5.7 eV. Both signals correspond to the oxidized component, Ti^{4+}.[11] From Fig. 1 it can be observed that there is no signal corresponding to either elemental titanium or other titanium sub-oxides. Therefore, it is clear from these Ti 2p photoemission spectra that the chemical state of titanium in the oxidized layer of the three alloys is mainly the oxidized Ti^{4+} state.

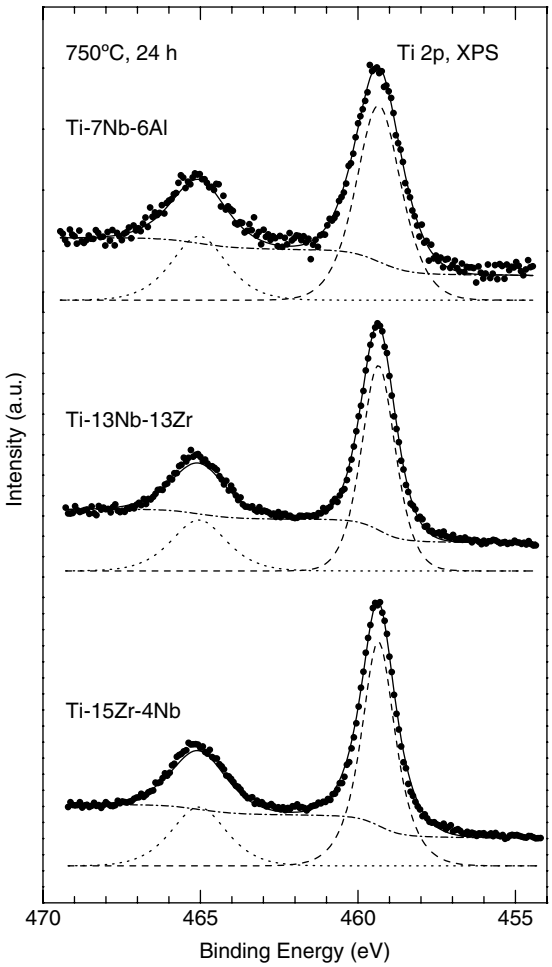

Figure 1. Ti 2p spectra of Ti–7Nb–6Al, Ti–13Nb–13Zr and Ti–15Zr–4Nb oxidized at 750 °C for 24 h. The dashed sub-spectra represent the $2p_{3/2}$ emissions for Ti^{4+} and the dotted sub-spectra represent the corresponding $2p_{1/2}$ emissions.

Figure 2 represents the Nb 3d emission, where the same procedure was applied. For the Ti–7Nb–6Al oxidized alloy no Nb 3d emission could be detected, indicating the absence of Nb oxides at the surface of the oxide layer. For the two TiNbZr oxidized alloys, the sub-spectra located at 207.5 eV BE, represented by the dashed curve, correspond to the Nb $3d_{5/2}$ emission and the sub-spectra located at 210.2 eV BE show the Nb $3d_{3/2}$ signal. Both emissions clearly indicate that the chemical state of Nb in both oxidized layers is Nb^{5+}.[11]

Al 2p emission from the Ti–7Nb–6Al oxidized alloy and Zr 3d emission from the two TiNbZr oxidized alloys were also measured by XPS (not shown). For Ti–7Nb–6Al, the Al 2p emission corresponded to the Al^{3+} oxidized state and for both TiNbZr alloys, the Zr 3d signal corresponded to the Zr^{4+} oxidized state.

Table 1 shows the quantitative surface atomic composition of the three oxidized Ti alloys as obtained from the analysis of the XPS spectra. As mentioned above, for all alloying elements the XPS analysis showed only the presence of the higher oxidation state, i.e., Ti^{4+}, Al^{3+}, Nb^{5+} and Zr^{4+}, without the presence of other sub-oxides or elemental

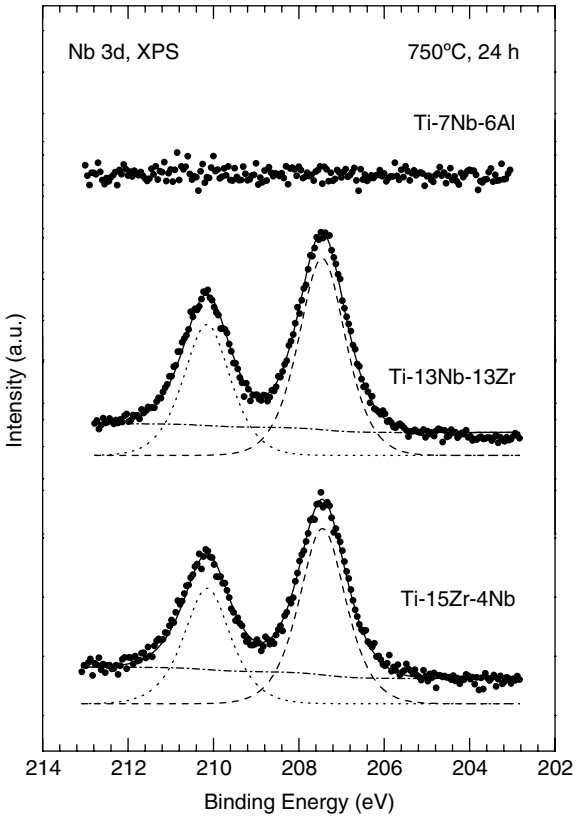

Figure 2. Nb 3d spectra of Ti–7Nb–6Al, Ti–13Nb–13Zr and Ti–15Zr–4Nb oxidized at 750 °C for 24 h. The dashed sub-spectra represent the $3d_{5/2}$ emissions for Nb^{5+} and the dotted sub-spectra represent the corresponding $3d_{3/2}$ emissions.

Table 1. Atomic percentage of the alloying elements at the surface of the oxide layer of Ti–6Al–7Nb, Ti–13Nb–13Zr and Ti–15Zr–4Nb after heat treatment at 750 °C for 24 h, as obtained from the XPS analysis

Alloys Oxidized at 750 °C for 24 h	at. %			
	Ti (Ti^{4+})	Al (Al^{3+})	Nb (Nb^{5+})	Zr (Zr^{4+})
Ti–6Al–7Nb	13 ± 3	87 ± 3	—	—
Ti–13Nb–13Zr	71 ± 3	—	26 ± 2	3 ± 1
Ti–15Zr–4Nb	80 ± 3	—	15 ± 2	5 ± 1

components. This is the expected result for the formation of stable oxide layers at elevated temperatures. According to the atomic composition shown in Table 1, there is a Nb surface enrichment for the TiNbZr alloys, whereas both Ti and Zr intensities decrease with respect to the bulk composition. In the case of the Ti–6Al–7Nb, the decrease of Ti is much more pronounced (from 86% in the bulk to 13% at the surface of the oxide layer). But in this case it is Al the element that segregates at the surface, increasing from 10.5% to 87% after oxidation. Surprisingly, no Nb is observed at the surface. This illustrates the different oxidation kinetics of the alloys. The diffusion of ionic species inside the oxide layer during the high-temperature treatment must play an important role, even more important than other thermodynamic considerations.[12]

To get more insight into the oxidation mechanisms, we have performed RBS experiments. This non-destructive technique can give information on the in-depth composition up to probing depths of the order of micrometres. Previous SEM studies[6] revealed a thickness of approximately 2, 10 and 25 μm for the oxidized Ti–7Nb–6Al, Ti–13Nb–13Zr and Ti–15Zr–4Nb alloys, respectively. Thus, the probing depth of RBS seems to be very suitable for the study of these oxide layers. To illustrate this, we show in Fig. 3 the elemental depth profile of the Ti–7Nb–6Al oxidized sample obtained after fitting the RBS and ERD data assuming two in-depth concentration levels separated by a variable-width boundary. The thickness of the oxide layer can be taken as the boundary position between inner and outer oxygen concentration levels. As can be seen in Fig. 3, this boundary is centred at $\sim 1.6 \times 10^{19}$ at/cm^2, which approximately corresponds to 2.5 μm, being in agreement with previous SEM observations. Figure 3 also shows Al surface segregation as well as Nb depletion. These observations agree with the XPS results commented on above, and can help the understanding of the formation of the oxide layer. The maximum Al content at the surface determined by RBS is lower than that observed by XPS, but this can be explained by the large difference in probing depth between both techniques, XPS being much more surface sensitive. Al segregation depth extends over approximately 0.5 μm. RBS results on TiNbZr alloys also show a good correlation with XPS data. A more detailed analysis will be published elsewhere.

In order to characterize the surface topography of the oxide layers formed on these alloys, AFM was performed on the three oxidized samples. As an example, Fig. 4 shows a representative AFM image of the surface of the Ti–7Nb–6Al oxidized alloy. This figure exhibits a regular surface topography with granular structure. The roughness, given by the root-mean-square value taken over several images, is ~200 nm for this oxidized alloy. AFM images of the Ti–13Nb–13Zr and Ti–15Zr–4Nb oxidized alloys give mean roughness values of 120 and 220 nm,

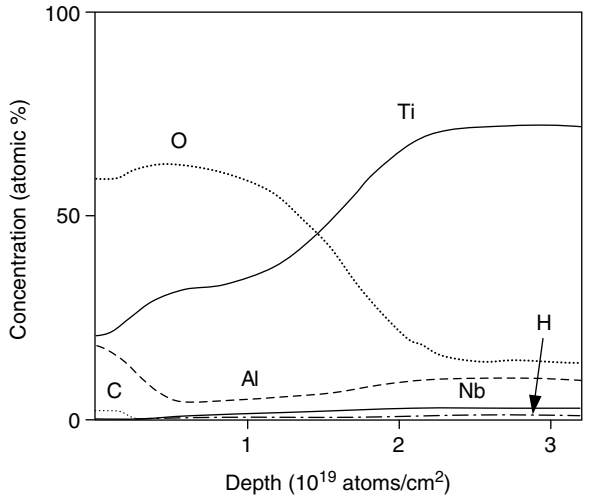

Figure 3. Element concentration depth profile as obtained by RBS for the Ti–7Nb–6Al alloy oxidized at 750 °C for 24 h.

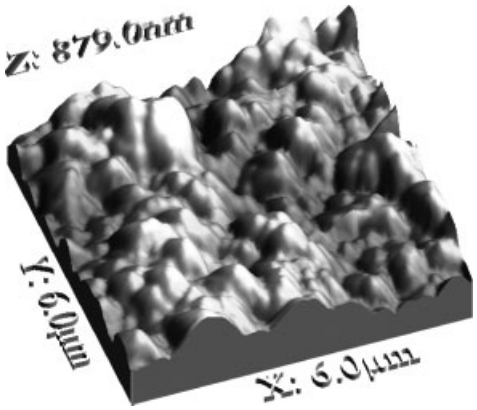

Figure 4. AFM topographic image of Ti–7Nb–6Al oxidized at 750 °C for 24 h.

respectively. The topography of the Ti–15Zr–4Nb alloy is quite irregular,[13] making this alloy not very convenient for biomedical applications. On the other hand, the more regular topography and large roughness of the oxidized Ti–7Nb–6Al alloy make it the most appropriate for these applications.

CONCLUSIONS

The surface composition and topography of three vanadium-free titanium alloys oxidized at 750 °C for 24 h were studied by XPS, RBS-ERD and AFM. For Ti–13Nb–13Zr and Ti–15Zr–4Nb oxidized alloys, the surface was composed mainly of TiO_2, with smaller amounts of Zr and Nb oxides. In both cases an enrichment of Nb at the surface is observed with respect to the bulk composition. The Ti–7Nb–6Al oxidized alloy shows a large increase of the Al concentration at the surface, and an absence of Nb. RBS measurements confirm these results and give an estimate for the Al segregation depth of about 0.5 µm. Finally, the AFM images exhibit for the oxidized Ti–7Nb–6Al alloy a more regular surface topography than the two Ti–Nb–Zr oxidized alloys.

Acknowledgements

This work has been supported by the Spanish *Programa de Tecnología de los Materiales de la Comunidad Autónoma de Madrid*, project 07N-0050-1999. A.G. thanks the Spanish *Ministerio de Ciencia y Tecnología* for financial support through the 'Ramón y Cajal' Program. F.P. acknowledges the Spanish *Ministerio de Educación, Cultura y Deporte* for financial support through a Sabbatical Year Grant (ref. SAB2000-0243).

REFERENCES

1. Kohn DH, Ducheyne P. In *Materials for Bone and Joint Replacement, Medical and Dental Materials. Serie Materials Science and Technology*, vol. 14. Williams DF (Ed.). VCH: Weinheim, 1992; 31–56.
2. Breme HJ, Biehl V, Helsen JA. In *Metals and Implants. Metals as Biomaterials*. Helsen JA, Breme HJ (Eds). Wiley: Chichester, 1998; 37–72.
3. Okazaki Y, Rao S, Ito Y, Tateishi T. *Biomaterials* 1998; **19**: 1197.
4. Sjoberg SG. *Acta Med. Scand.* 1956; **154**: 381.
5. Lin DJ, Chern Lin JH, Ju CP. *Biomaterials* 2002; **23**: 1723.
6. López MF, Gutiérrez A, Jiménez JA. *Electrochim. Acta* 2003; **48**: 1395.
7. López MF, Gutiérrez A, Jiménez JA. *Electrochim. Acta* 2002; **47**: 1359.
8. Lopez MF, Gutiérrez A, Jiménez JA. *Surf. Sci.* 2001; **482–485**: 300.
9. Kótai E. *Nucl. Instrum. Methods* 1994; **B85**: 588.
10. Nanotec Electronica, http://www.nanotec.es
11. Moulder JF, Stickle WF, Sobol PE, Bomben KD. In *Handbook of X-ray Photoelectron Spectroscopy*. Chastain J (Ed.). Perkin-Elmer: Minnesota, 1992.
12. López MF, Soriano L, Palomares FJ, Sánchez-Agudo M, Fuentes GG, Gutiérrez A, Jiménez JA. *Surf. Interface Anal.* 2002; **33**: 570.
13. Morant C, López MF, Gutiérrez A, Jiménez JA. *Appl. Surf. Sci.* 2003; **220**: 79.